J|A|C|S
ARTICLES
Published on Web 06/03/2003

Bis(μ-oxo)dicopper in Cu-ZSM-5 and Its Role in the Decomposition of NO: A Combined in Situ XAFS, UV−Vis−Near-IR, and Kinetic Study

Marijke H. Groothaert,[†] Jeroen A. van Bokhoven,[‡,§] Andrea A. Battiston,[‡] Bert M. Weckhuysen,[‡] and Robert A. Schoonheydt*,[†]

Contribution from the Center for Surface Chemistry and Catalysis, Katholieke Universiteit Leuven, Kasteelpark Arenberg 23, B-3001 Leuven, Belgium, and the Department of Inorganic Chemistry and Catalysis, Debye Institute, Utrecht University, Sorbonnelaan 16, 3584 CA Utrecht, The Netherlands

Received December 11, 2002; E-mail: Robert.Schoonheydt@agr.kuleuven.ac.be

Abstract: In situ XAFS combined with UV−vis−near-IR spectroscopy are used to identify the active site in copper-loaded ZSM-5 responsible for the catalytic decomposition of NO. Cu−ZSM-5 was probed with in situ XAFS (i) after O_2 activation and (ii) while catalyzing the direct decomposition of NO into N_2 and O_2. A careful *R*-space fitting of the Cu K-edge EXAFS data is presented, including the use of different *k*-weightings and the analysis of the individual coordination shells. For the O_2-activated overexchanged Cu−ZSM-5 sample a Cu···Cu contribution at 2.87 Å with a coordination number of 1 is found. The corresponding UV−vis−near-IR spectrum is characterized by an intense absorption band at 22 700 cm^{-1} and a relatively weaker band at 30 000 cm^{-1}, while no corresponding EPR signal is detected. Comparison of these data with the large databank of well-characterized copper centers in enzymes and synthetic model complexes leads to the identification of the bis(μ-oxo)dicopper core, i.e. $[Cu_2(\mu\text{-}O)_2]^{2+}$. After dehydration in He, Cu−ZSM-5 shows stable NO decomposition activity and the in situ XAFS data indicate the formation of a large fraction of the bis(μ-oxo)dicopper core during reaction. When the Cu/Al ratio of Cu−ZSM-5 exceeds 0.2, both the bis(μ-oxo)dicopper core is formed and the NO decomposition activity increases sharply. On the basis of the in situ measurements, a reaction cycle is proposed in which the bis(μ-oxo)dicopper core forms the product O_2 on a single active site and realizes the continuous O_2 release and concomitant self-reduction.

1. Introduction

The simplest and most desirable approach to NO abatement is the direct decomposition of NO into N_2 and O_2.[1] This reaction is thermodynamically favored at temperatures below 1000 K,[2] but to date no stable catalyst with a continuously high conversion suitable for industrial implementation has been reported. The discovery of the uniquely high activity of the overexchanged (Cu/Al > 0.5) Cu−ZSM-5 zeolite by Iwamoto and co-workers[3] in 1986 was a significant breakthrough in this field of research. The most important limitations of Cu−ZSM-5 for practical application are (i) a too low activity by 1−2 orders of magnitude and (ii) the suppression of the activity by water vapor and SO_2.[2] Nowadays, several research groups study modifications of Cu−ZSM-5, e.g. by adding a second cation or altering the support,[4,5] in order to increase the activity and stability. Alternatively, much research has focused on the active sites in Cu−ZSM-5 and the reaction mechanism, since this information may also indicate ways to design more active catalysts.

It is well-established that the NO decomposition activity has an S-shaped dependence on the copper exchange level in ZSM-5.[1,6,7] The NO decomposition rate gradually increases for the lower exchange levels and increases sharply above the Cu/Al ratio of 0.2.[6] This finding is explained in the literature by the following two conflicting interpretations:

(1) The ZSM-5 zeolite has two or more types of isolated copper cation sites, and the catalytically most active site is less favorable for cation exchange.[8,9] In line with this interpretation it is assumed that in the highly loaded samples, $[Cu^{2+}(OH)^-]^+$ ions are exchanged close to one framework aluminum.[10] Upon dehydration, isolated $Cu^{2+}O^-$ and Cu^+ ions are created from two $[Cu^{2+}(OH)^-]^+$ ions by expelling one H_2O molecule (eq 1).[11]

[†] Katholieke Universiteit Leuven.
[‡] Utrecht University.
[§] Current address: Institute for Chemical and Bioengineering, ETH Hönggerberg HCI, CH-8093 Zürich, Switzerland.

(1) Yahiro, H.; Iwamoto, M. *Appl. Catal. A* **2001**, *222*, 163.
(2) Shelef, M. *Chem. Rev.* **1995**, *95*, 209.
(3) Iwamoto, M.; Furukawa, H.; Mine, Y.; Uemura, F.; Mikuriya, S. I.; Kagawa, S. *J. Chem. Soc., Chem. Commun.* **1986**, 1272.
(4) Dedecek, J.; Bortnovsky, O.; Vondrová, A.; Wichterlová, B. *J. Catal.* **2001**, *200*, 160.
(5) Pârvulescu, V. I.; Grange, P.; Delmon, B. *Appl. Catal. B* **2001**, *33*, 223.
(6) Iwamoto, M.; Yahiro, H.; Tanda, K.; Mizuno, N.; Mine, Y.; Kagawa, S. *J. Phys. Chem.* **1991**, *95*, 3727.
(7) Centi, G.; Perathoner, S. *Appl. Catal. A* **1995**, *132*, 179.
(8) Wichterlová, B.; Dedecek, J.; Sobalík, Z.; Vondrová, A.; Klier, K. *J. Catal.* **1997**, *169*, 194.
(9) Dedecek, J.; Wichterlová, B. *Phys. Chem. Chem. Phys.* **1999**, *1*, 629.
(10) Dedecek, J.; Wichterlová, B. *J. Phys. Chem. B* **1997**, *101*, 10233.

$$2[Cu^{2+}(OH)^{-}]^{+} \rightarrow Cu^{2+}O^{-} + Cu^{+} + H_2O \qquad (1)$$

Wichterlová and co-workers suggested that the Cu^{+} ions balanced by a single framework aluminum, with a characteristic photoluminescence band at 540 nm, are responsible for the high NO decomposition activity.[9] An energetically plausible mechanism for NO decomposition on an isolated copper ion has been proposed in a computational study of Schneider et al.[12] Essentially, it comes down to the adsorption of two NO molecules on Cu^{+}, which results in the formation of N_2O and $Cu^{2+}O^{-}$. $Cu^{2+}O^{-}$ can further react with N_2O, causing first the liberation of N_2 and then O_2 via $Cu^{2+}O_2^{-}$. Earlier, Liu and Robota found in their in situ XANES (X-ray absorption near-edge structure) experiments that the Cu(I) ion signal intensity of the Cu−ZSM-5 sample correlated well with the NO decomposition rate.[13] However, the latter finding does not necessarily infer the presence of isolated copper ions and leads us to the second interpretation of the S-shaped dependence of the activity on the copper exchange level.

(2) The NO decomposition proceeds only under cooperation of two adjacent copper atoms, which can be formed at high exchange levels.[14−16] Therefore two $[Cu^{2+}(OH)^{-}]^{+}$ ions are thought to condense first in a $Cu^{2+}-O^{2-}-Cu^{2+}$ oxocation and then a $Cu^{+}\cdots Cu^{+}$ pair upon high-temperature treatment in He (eq 2).[17,18]

$$2[Cu^{2+}(OH)^{-}]^{+} \rightarrow Cu^{2+}-O^{2-}-Cu^{2+} + H_2O \qquad (2a)$$

$$2Cu^{2+}-O^{2-}-Cu^{2+} \rightarrow 2Cu^{+}\cdots Cu^{+} + O_2 \qquad (2b)$$

Anpo et al. assigned the photoluminescence band around 540 nm to $Cu^{+}\cdots Cu^{+}$ dimers,[19] which is in contrast to the assignment of Wichterlová and co-workers.[9] On the basis of mass spectrometric analysis of the amount of oxygen removed during thermal treatments, Iglesia and co-workers[16] determined that 78% of the copper content in O_2-treated Cu−ZSM-5 (Cu/Al = 0.6) is present as $Cu^{2+}-O^{2-}-Cu^{2+}$. Using DRS (diffuse reflectance spectroscopy), a strong absorption band at about 22 700 cm^{-1} [20−23] and eventually at 31 200 cm^{-1} [21] is observed for the overexchanged O_2-treated Cu−ZSM-5. In accordance with interpretation (2), all authors associate this electronic absorption spectrum with the presence of a single-O bridged copper pair. Teraoka et al.[23] stress that the latter copper pair has a mixed valency in that the extra-lattice-oxygen atom bridges a Cu^{2+} and a Cu^{+}. The catalytic NO decomposition cycle on copper dimers, proposed in an IR study of Iwamoto and co-workers,[1,15] starts with the adsorption of two NO molecules on $Cu^{+}\cdots Cu^{+}$. N_2O is produced together with a $Cu^{2+}-O^{2-}-Cu^{2+}$ oxocation, which reconstitutes the $Cu^{+}\cdots Cu^{+}$ pair above 573 K by the desorption of $^1/_2$ O_2. According to Iglesia and co-workers, the intermediate N_2O also reacts with $Cu^{+}\cdots Cu^{+}$ to produce N_2 and $Cu^{2+}-O^{2-}-Cu^{2+}$.[24] In a quite recent DFT (density functional theory) contribution of Goodman et al.[25] it was stressed that not only single-O bridged but also a variety of double-O bridged Cu pairs are highly stable for conditions likely to exist in Cu−ZSM-5. On the basis of this knowledge, $[CuO_2Cu]^{2+}$ has been included in some recent NO decomposition cycles[24,26,27] and is proposed to play a role in O_2 formation, either directly via the release of O_2 or indirectly via recombinative desorption requiring vicinal oxocations or NO-mediated oxygen removal. However, none of the double-O bridged copper pairs that are proposed in the theoretical contribution of Goodman et al.[25] have been identified spectroscopically so far.

The formation of copper pairs in ZSM-5 is also supported by several EXAFS (extended X-ray absorption fine structure) studies. Hamada et al.[28] were the first to suggest the contribution of a Cu···Cu local structure in the EXAFS spectra of typical overexchanged samples, active for NO decomposition. Using fitting techniques, Grünert et al.[29] deduced a Cu···Cu distance of 2.95 Å from the EXAFS data of O_2-treated and evacuated overexchanged samples and assigned it to small clusters with the copper atoms linked by extra-lattice-oxygen species. Kuroda et al.[30] and Palomino et al.[17] assigned the contribution at about 2.75 Å in their EXAFS spectra of evacuated highly exchanged samples to the presence of $Cu^{+}\cdots Cu^{+}$ pairs. In contrast, other EXAFS studies of overexchanged Cu−ZSM-5 samples revealed no Cu···Cu interaction.[31,32] One of the reasons for this discrepancy in the literature might be the different method of Cu introduction in ZSM-5. Moreover, in these EXAFS studies, NO decomposition activity was not reported, except for the study of Hamada et al.[28]

In the present contribution, Iwamoto's method[33] using copper(II) acetate was followed to prepare overexchanged Cu−ZSM-5 samples. The samples showed the stable NO decomposition activity as reported by Iwamoto et al.[6] In situ XAFS measurements were performed during the reaction, and the analysis of the EXAFS data is based on a careful fitting procedure. Analysis of Cu K-edge EXAFS on systems containing heavy and light scatterers has proven to be difficult, but a systematic and careful analysis provides detailed information.[34] This study also presents

(11) Larsen, S. C.; Aylor, A.; Bell, A. T.; Reimer, J. A. *J. Phys. Chem.* **1994**, *98*, 11533.
(12) Schneider, W. F.; Hass, K. C.; Ramprasad, R.; Adams, J. B. *J. Phys. Chem. B* **1998**, *102*, 3692.
(13) Liu, D. J.; Robota, H. J. *Catal. Lett.* **1993**, *21*, 291.
(14) Lei, G. D.; Adelman, B. J.; Sárkány, J.; Sachtler, W. M. H. *Appl. Catal. B* **1995**, *5*, 245.
(15) Iwamoto, M.; Yahiro, H.; Mizuno, N.; Zhang, W. X.; Mine, Y.; Furukawa, H.; Kagawa, S. *J. Phys. Chem.* **1992**, *96*, 9360.
(16) Da Costa, P.; Moden, B.; Meitzner, G. D.; Lee, D. K.; Iglesia, E. *Phys. Chem. Chem. Phys.* **2002**, *4*, 4590.
(17) Palomino, G. T.; Fisicaro, P.; Bordiga, S.; Zecchina, A.; Giamello, E.; Lamberti, C. *J. Phys. Chem. B* **2000**, *104*, 4064.
(18) Sárkány, J.; D'Itri, J. L.; Sachtler, W. M. H. *Catal. Lett.* **1992**, *16*, 241.
(19) Anpo, M.; Matsuoka, M.; Shioya, Y.; Yamashita, H.; Giamello, E.; Morterra, C.; Che, M.; Patterson, H. H.; Webber, S.; Ouellette, S.; Fox, M. A. *J. Phys. Chem.* **1994**, *98*, 5744.
(20) Itho, Y.; Nishiyama, S.; Tsuruya, S.; Masai, M. *J. Phys. Chem.* **1994**, *98*, 960.
(21) Praliaud, H.; Mikhailenko, S.; Chajar, Z.; Primet, M. *Appl. Catal. B* **1998**, *16*, 359.
(22) de Carvalho, M.; Passos, F. B.; Schmal, M. *Appl. Catal. A* **2000**, *193*, 265.
(23) Teraoka, Y.; Tai, C.; Ogawa, H.; Furukawa, H.; Kagawa, S. *Appl. Catal. A* **2000**, *200*, 167.
(24) Moden, B.; Da Costa, P.; Fonfe, B.; Lee, D. K.; Iglesia, E. *J. Catal.* **2002**, *209*, 75.
(25) Goodman, B. R.; Schneider, W. F.; Hass, K. C.; Adams, J. B. *Catal. Lett.* **1998**, *56*, 183.
(26) Moden, B.; Da Costa, P.; Lee, D. K.; Iglesia, E. *J. Phys. Chem. B* **2002**, *106*, 9633.
(27) Konduru, M. V.; Chuang, S. S. C. *J. Catal.* **2000**, *196*, 271.
(28) Hamada, H.; Matsubayashi, N.; Shimada, H.; Kintaichi, Y.; Ito, T.; Nishijima, A. *Catal. Lett.* **1990**, *5*, 189.
(29) Grünert, W.; Hayes, N. W.; Joyner, R. W.; Shpiro, E. S.; Siddiqui, M. R. H.; Baeva, G. N. *J. Phys. Chem.* **1994**, *98*, 10832.
(30) Kuroda, Y.; Kumashiro, R.; Yoshimoto, T.; Nagao, M. *Phys. Chem. Chem. Phys.* **1999**, *1*, 649.
(31) Yamashita, H.; Matsuoka, M.; Tsuji, K.; Shioya, Y.; Anpo, M.; Che, M. *J. Phys. Chem.* **1996**, *100*, 397.
(32) Lamberti, C.; Bordiga, S.; Salvalaggio, M.; Spoto, G.; Zecchina, A.; Geobaldo, F.; Vlaic, G.; Bellatreccia, M. *J. Phys. Chem. B* **1997**, *101*, 344.
(33) Iwamoto, M.; Yahiro, H.; Mine, Y.; Kagawa, S. *Chem. Lett.* **1989**, 213.
(34) Tromp, M.; van Bokhoven, J. A.; Arink, A. M.; Bitter, J. H.; van Koten, G.; Koningsberger, D. C. *Chem.-Eur. J.* **2002**, *8*, 5667.

Table 1. Summary of the Pretreatments and Measurements of the Different Samples

sample	Pretreatment	catalysis	XAFS	DRS	EPR
CZ-31−0.16	5 K min^{-1} to 623 K and 3 h at 623 K in O_2			(RT)[a]	(LN)[b]
CZ-31−0.34	5 K min^{-1} to 623 K and 3 h at 623 K in O_2			(RT)	(LN)
CZ-31−0.58	5 K min^{-1} to 623 K and 3 h at 623 K in O_2		(LN)	(RT)	(LN)
CZ-12−0.62	5 K min^{-1} to 623 K and 3 h at 623 K in O_2		(LN)	(RT)	(LN)
CZ-12−0.62	10 K min^{-1} to 393 K and 30 min at 393 K in He		(LN)		
CZ-12−0.62	(a) 10 K min^{-1} to 773 K and 2 h at 773 K in He		(773 K)		
	(b) = (a) + 2 h at 773 K in He + 1 h at 773 K in NO/He		(773 K)		
	(c) = (b) + 1 h at 773 K in NO/He		(LN)		
CZ-12−0.62	5 K min^{-1} to 773 K and 4 h at 773 K in He, + NO/He	(773−523 K)			
CZ-31−0.58	5 K min^{-1} to 773 K and 4 h at 773 K in He, + NO/He	(773−523 K)			

[a] RT = room temperature. [b] LN = liquid N_2 temperature.

XAFS, UV−vis−near-IR, and EPR (electron paramagnetic resonance) data of O_2-activated Cu−ZSM-5 samples. For the first time, these data will be interpreted with the aid of well-characterized copper core structures in enzymes and synthetic model complexes.

2. Experimental Section

2.1. Samples. A parent K−ZSM-5 with Si/Al = 31 was kindly supplied by ExxonMobil Chemical, and a Na−ZSM-5 with Si/Al = 12 was obtained from ALSI-PENTA. K−ZSM-5 was put in the Na^+-form and the zeolites were overexchanged with Cu^{2+} according to the method of Iwamoto et al.[33] A 1 g amount of ZSM-5 was ion-exchanged in 25 mL (for Si/Al = 31) or 63 mL (for Si/Al = 12) of a 0.01 M $Cu(CH_3CO_2)_2 \cdot H_2O$ solution overnight at ambient temperature. After filtration, the obtained wet cake was again ion-exchanged in new copper solution, and after three ion-exchange treatments the zeolite was washed and dried at 383 K. Two underexchanged Cu(II) samples were prepared by adding 1 g of ZSM-5 (Si/Al = 31) and 100 mL of respectively 1 mM and 2.5 mM $Cu(NO_3)_2 \cdot 3H_2O$ to 900 mL of water. The slurries were vigorously stirred at ambient temperature while the pH was kept in the range between 5 and 5.2. After 24 h of exchange the zeolite samples were filtered, washed, and dried. The Cu and Al contents of the samples were determined by inductively coupled plasma (ICP). The as-prepared Cu−ZSM-5 samples will be denoted as CZ-*X*−*Y*, where *X* gives the Si/Al ratio and *Y* the Cu/Al ratio. Table 1 summarizes the samples and the respective pretreatments and measurements.

2.2. Catalytic Testing. The Cu−ZSM-5 materials were tested for the decomposition of NO in a plug-flow reactor (i.d. = 1.2 cm). A 0.5 g amount of the sample (pellets of 90−150 μm) was diluted with 5 g of quartz (Fluka Chemika) and loaded in the reactor. The sample was preheated to 773 K in a He flow of 50 mL min^{-1}, as indicated in Table 1. The reaction feed was obtained by blending two flows, i.e. 1 mol % NO in He and the balance He. The resulting inlet for the NO decomposition was 1000 ppm NO (=0.1 mol % NO) in He, with an overall flow of 15 mL min^{-1}. Based on an apparent zeolite density of 0.5 g cm^{-3}, the calculated gas hourly space velocity (GHSV) was 900 h^{-1} (W/F = 2.0 g s cm^{-3}). A Perkin-Elmer Autosystem XL gas chromatograph (GC) equipped with a TCD detector was used to monitor the effluent N_2, O_2, and N_2O. To be able to measure NO and NO_2, a Thermo Environmental Instruments 42C NO_x chemiluminescence analyzer was connected in parallel with the GC. The GC and the NO_x analyzer could be operated simultaneously. The activity of the samples was tested as a function of the temperature. In Figure 1a the reactor outlet composition of CZ-12−0.62 at each temperature is shown and the balances for N and O in the outlet fall in the range of 984−1016 ppm at each temperature. This shows that the mass balance is complete. These data of the reactor outlet composition were used to calculate the N- and O-selectivities as exemplified in eq 3 for NO_2.

$$\text{N-selectivity toward } NO_2\ (\%) = \frac{(\text{ppm } NO_2 \text{ in outlet}) \times 100}{1000 - (\text{ppm NO in outlet})}$$

$$\text{O-selectivity toward } NO_2\ (\%) = \frac{2(\text{ppm } NO_2 \text{ in outlet}) \times 100}{1000 - (\text{ppm NO in outlet})} \quad (3)$$

2.3. XAFS Data Collection. Cu K-edge absorption spectra were collected at beamline X1.1 of the HASYLAB, Hamburg (Germany), using a Si(111) double crystal monochromator. All measurements were performed in transmission mode using ionization chambers, filled with nitrogen (I_{zero}) and argon ($I_{transmitted}$). As an internal reference, a 7 μm thick Cu foil was simultaneously measured between the second and third ionization chambers. The energy scale was calibrated at the position of the main edge-jump of the Cu foil at 8979 eV. The monochromator was detuned to 50% of maximum intensity to reduce the interference of higher harmonics present in the X-ray beam. To minimize both high- and low-frequency noise, the counting time per data point was increased from 1 to 3 s from the beginning to the end of a scan. Energy steps were made in *k*-space, and three scans were averaged. Samples were pressed in self-supporting wafers and mounted in an in situ cell that allows temperature treatments while flowing a gas during data collection.[35] The cell was equipped with beryllium windows. The thickness of the wafer was chosen to give an absorption of $\mu_x = 2.5$ at the Cu absorption edge for an optimal signal-to-noise ratio. Typically, about 50−60 mg of catalyst was used. The pretreatments of the different samples are summarized in Table 1. Each XAFS measurement was performed on a fresh sample, except for sample CZ-12−0.62, which was submitted to three subsequent measurements as indicated in Table 1. The NO concentration was 2000 ppm, and in all cases the total flow was 50 mL min^{-1}.

2.4. XAFS Data Analysis. Data reduction and analysis were performed with the XDAP code using standard methods. The preedge was subtracted using a modified Victoreen curve,[36,37] and the background was subtracted using cubic spline routines.[38] Spectra were normalized by dividing the absorption intensity by the height of the absorption edge at 50 eV above the edge. To analyze the experimental XAFS data, Cu−O, Cu−Cu, and Cu−Al references were used to fit the respective contributions. EXAFS data from reference compounds were used to generate reference files for Cu−Cu (using a Cu foil) and for Cu−O (using copper phthallocyanine, since O and N are neighboring elements in the periodic table),[34] both measured at liquid nitrogen (LN) temperature. As no reference compound was available for making a reference for Cu−Al, a theoretical reference using FEFF8 was produced, using default parameters.[39] The Debye−Waller factor and S_0^2 were set to 0 and 1, respectively, for this reference. As a consequence, the Debye−Waller factors for Cu−Al represent absolute values, whereas

(35) Kampers, F. W. H.; Maas, T. M. J.; van Grondelle, J.; Brinkgreve, P.; Koningsberger, D. C. *Rev. Sci. Instrum.* **1989**, *60*, 2635.
(36) Vaarkamp, M.; Dring, I.; Oldman, R. J.; Stern, E. A.; Koningsberger, D. C. *Phys. Rev. B: Condens. Matter Mater. Phys.* **1994**, *50*, 7872.
(37) van Zon, J. B. A. D.; Koningsberger, D. C.; van Blik, H. F. J.; Sayers, D. E. *J. Chem. Phys.* **1985**, *82*, 5742.
(38) Cook, J. W.; Sayers, D. E. *J. Appl. Phys.* **1981**, *52*, 5024.
(39) Ankudinov, A. L.; Ravel, B.; Rehr, J. J.; Conradson, S. D. *Phys. Rev. B: Condens. Matter Mater. Phys.* **1998**, *58*, 7565.

Table 2. Summary of XANES Assignments

peak assignment	energy at peak maximum (eV)	peak assignment	energy at peak maximum (eV)
Cu(II) 1s → 3d	8976−8979	two-coordinate Cu(I) along *z*-axis:	
Cu(II) 1s → 4p	8995−8998	Cu(I) 1s → $4p_{x,y}$	8982−8984
tetragonal Cu(II) elongated along *z*-axis:		three-coordinate Cu(I) in *yz* plane:	
Cu(II) 1s → $4p_z$ + L → Cu(II) shakedown	8985−8988	Cu(I) 1s → $4p_x$	8982−8984
Cu(I) 1s → 4p	8993−8995	Cu(0)	8982

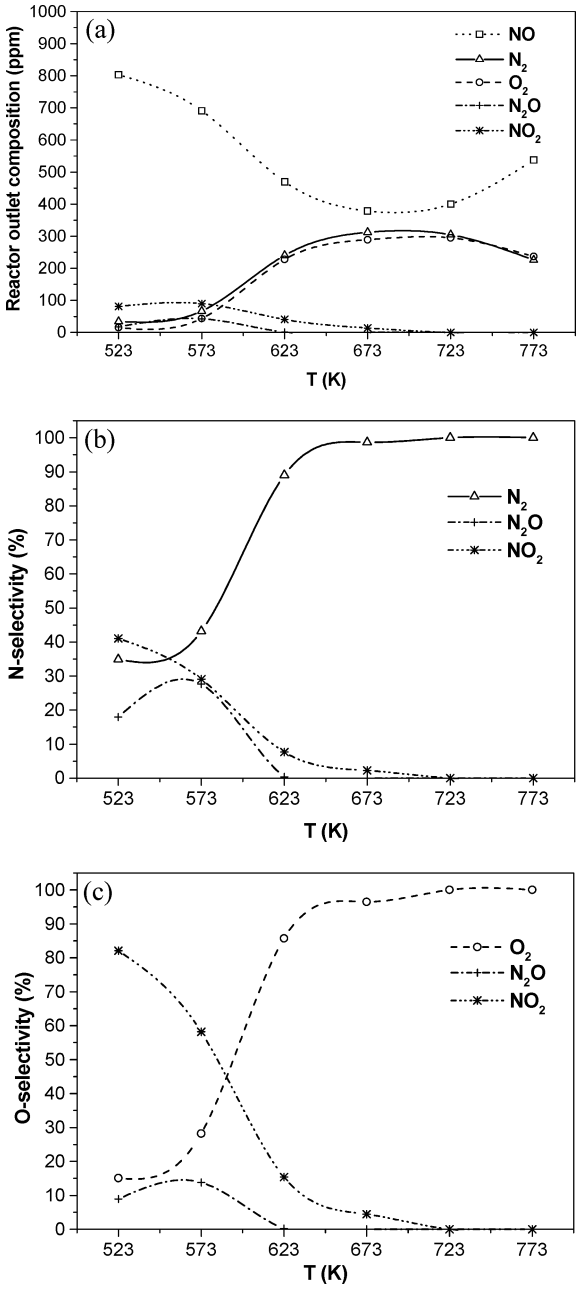

Figure 1. (a) Reactor outlet composition of CZ-12−0.62 contacted with 1000 ppm NO in He at 900 h^{-1}; (b) the corresponding N-selectivity and (c) O-selectivity (all as a function of temperature).

for the Cu−Cu and Cu−O contributions they are relative values compared to the reference compounds. Data analysis was performed by multiple shell fitting in *R*-space. Using the difference file technique, all single contributions were closely observed and tested for significance toward the level of noise. All fits were performed using k^2-weighted Fourier transforms, and a fit is only accepted if fits of k^0- and k^3-weighted Fourier transforms are of equal quality. The errors in the fit parameters were estimated to be 10−20% in coordination number (*N*), 1−2% in distance (*R*), 5% in Debye−Waller factor ($\Delta\sigma^2$), and 10% in inner potential correction (ΔE_0).

2.5. EPR and DRS. The samples were pelletized (0.25−0.4 mm) and brought into quartz flow cells, which have a suprasil window for DRS measurements and a quartz sidearm for EPR measurements. The samples were treated in flowing O_2 (50 mL min^{-1}) according to the temperature profile given in Table 1. After cooling the samples in O_2 and flushing the samples with He for 60 s at room temperature (RT), X-band EPR spectra were recorded at LN with a Bruker ESP 300E instrument in a rectangular TE_{104} cavity. Spin concentrations were calculated by double integration of the first derivative spectra and comparison with KCl diluted $Cu(acac)_2$ standards of known spin concentration (acac = acetylacetonate). The absolute margin of error on the calculated spin concentrations is estimated below 20%.[40] DRS spectra were recorded on a Varian Cary 5 UV−vis−near-IR spectrophotometer at RT.

3. Results

3.1. NO Decomposition Activity. Figure 1a presents the composition of the outlet of CZ-12−0.62 contacted with 1000 ppm NO in He, as a function of the reactor temperature. Additionally, the corresponding N- and O-selectivities are plotted in Figure 1b,c. The data will be discussed in order of decreasing temperature, conforming to the experimental performance. In the temperature range from 773 to 723 K a 100% selective NO decomposition to O_2 and N_2 was obtained. At 673 K the conversion of NO attains its highest value of 62%, but the selectivity is slightly below 100% as a small fraction of NO_2 is observed. Below 573 K, both the activity and selectivity of the NO decomposition significantly drop. NO_2 is then the major product, while N_2O attains its highest level at 573 K. To the best of our knowledge, this is the first report of a near 100% selective decomposition of NO to N_2 and O_2 over Cu−ZSM-5 for a 0.1 mol % NO flow. This high selectivity may be correlated with the lower NO concentrations applied compared to other studies.[1,6,41,42] Indeed, increased O_2 formation resulting from higher NO concentrations is suggested to additionally produce NO_2 ($O_2 + 2NO \rightarrow 2NO_2$), whether in the reactor itself or in the colder parts of the GC.[1,43] Hence, lower selectivities were reported in these studies, which were confirmed in our laboratories. Regarding the CZ-31−0.58 sample characterized by a higher Si/Al ratio, the obtained N- and O-selectivities are very similar to the results presented for CZ-12−0.62. The TOF (molecules NO converted to N_2 per second per Cu atom) at 0.1 mol % NO and 673 K was about 2.3 times higher for CZ-31−0.58 than for CZ-12−0.62 with values of 3.7×10^{-5} and 1.6×10^{-5} s^{-1}, respectively.

3.2. Cu K-Edge XANES. Examination of the XANES spectra provides direct information on the oxidation state of copper.

(40) Weckhuysen, B. M.; Schoonheydt, R. A. In *Spectroscopy of Transition Metal Ions on Surfaces*; Weckhuysen, B. M., Van Der Voort, P., Catana, G., Eds.; Leuven University Press: Leuven, Belgium, 2000; p 25.
(41) Li, Y. J.; Hall, W. K. *J. Catal.* **1991**, *129*, 202.
(42) Ganemi, B.; Björnbom, E.; Paul, J. *Appl. Catal. B* **1998**, *17*, 293.
(43) Li, Y. J.; Hall, W. K. *J. Phys. Chem.* **1990**, *94*, 6145.

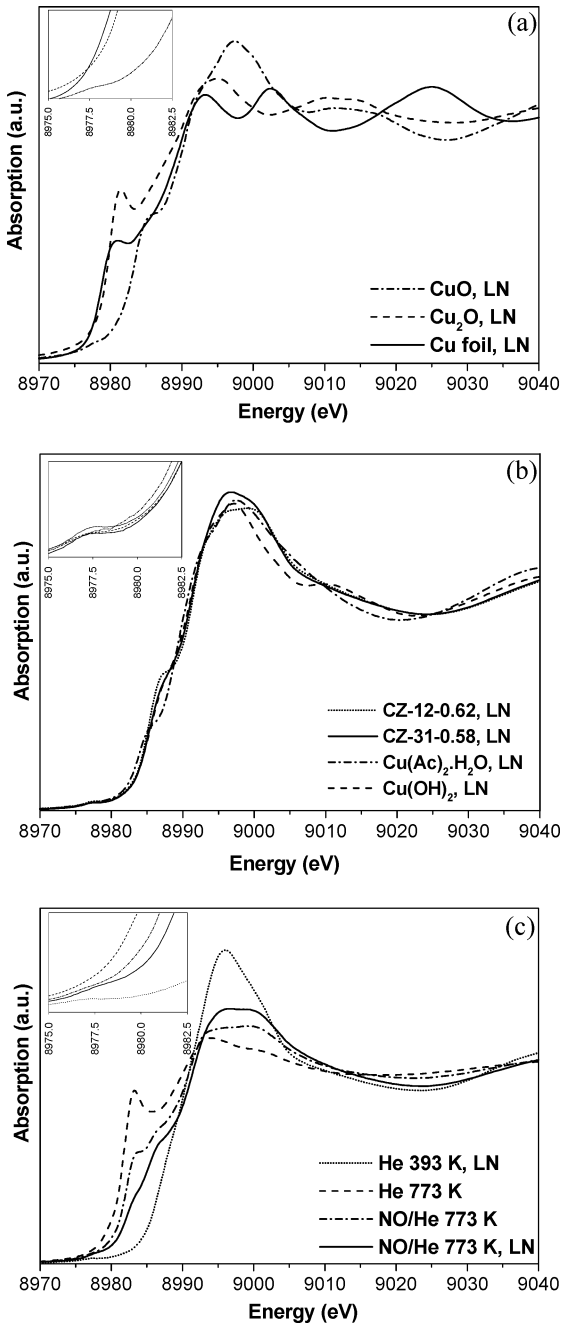

Figure 2. XANES spectra of (a) CuO, Cu_2O, and Cu foil at LN; (b) CZ-12−0.62 and CZ-31−0.58 treated in O_2 at 623 K and of copper(II) acetate monohydrate and $Cu(OH)_2$ measured at LN; (c) CZ-12−0.62 (i) treated in He at 393 K and measured at LN, (ii) treated in He at 773 K and measured at 773 K, (iii) treated in NO/He at 773 K and measured at 773 K, and (iv) treated in NO/He at 773 K and measured at LN.

The characteristic near-edge absorption features together with their interpretations are given in Table 2.[13,17,30−32,44−47]

These assignments can be illustrated with the XANES spectra of the model compounds CuO, Cu_2O, and Cu foil, depicted in Figure 2a. In the inset of Figure 2a a weak peak around 8977.5 eV can be distinguished for CuO. This peak corresponds to the dipole-forbidden Cu(II) 1s → 3d electronic transition and is recognized as the fingerprint of bivalent Cu. The dipole-allowed Cu(II) 1s → 4p transitions are located on the absorption edge at about 8995−8998 eV. In the case of tetragonal Cu(II) symmetry, as in CuO, the 1s → $4p_z$ transition shifts to lower energy, resulting in a clear shoulder at 8985.5 eV for CuO. According to Solomon and co-workers, the covalency of the ligands enhances the latter shift, and they assigned this peak at ∼8986 eV as the 1s → $4p_z$ transition with simultaneous ligand-to-Cu(II) charge transfer (CT) excitation.[46] In analogy, the 1s → 4p transitions of tetrahedral Cu(I) complexes are all above 8985 eV, whereas two- and three-coordinate Cu(I) complexes have a 1s → 4p absorption feature at 8982−8984 eV.[47] Cu(I) in Cu_2O possesses a linear two-coordinate structure, and consequently a sharp peak at 8982 eV is observed. Metallic Cu exhibits also a near-edge feature around 8982 eV. However, the resonance features above the edge jump are clearly different from those of Cu_2O, as can be seen in Figure 2a.

In Figure 2b, the XANES spectra of O_2-treated CZ-31−0.58 and CZ-12−0.62 are compared with the spectra of copper(II) acetate monohydrate and $Cu(OH)_2$. The Cu(II) 1s → 3d and Cu(II) 1s → $4p_z$ + L → Cu(II) transitions of the O_2-treated Cu(II) zeolite samples are positioned at respectively 8977.5 and 8987 eV and show a reasonably good match with those of $Cu(OH)_2$. This resemblance suggests a planar symmetry around Cu(II) in the O_2-treated Cu(II) zeolites, as in $Cu(OH)_2$. On the other hand, the resonance features above the edge jump in the spectra of the Cu(II) zeolites and $Cu(OH)_2$ are different which indicates that the atomic ordering around the Cu(II) ions in the zeolite deviates from that in the parallel chains of $Cu(OH)_2$. In Figure 2c the XANES spectra of the CZ-12−0.62 sample measured under different conditions are compared. The spectrum recorded after He pretreatment at 393 K exhibits the weak peak at 8977.5 eV, which is indicative of Cu(II). After He pretreatment at 773 K no intensity can be distinguished at 8977.5 eV and a sharp peak is formed at 8983 eV, providing evidence that the majority of the Cu(II) ions is reduced to Cu(I). Under NO decomposition conditions at 773 K, the Cu(I) peak at 8983 eV is reduced while a shoulder at 8987 eV is distinguished. The latter peak can be assigned to a Cu(II) 1s → $4p_z$ + L → Cu(II) shakedown and is positioned at energy equal to that in the O_2-treated sample (see Figure 2b). After prolonging the NO decomposition and cooling the sample to LN, the Cu(I) peak is even more reduced.

3.3. EXAFS Data Analysis Procedure. Several EXAFS contributions in catalysis research demonstrate the necessity of a systematic EXAFS data-analysis strategy for an unbiased interpretation.[34,48] Therefore, the fitting strategy in *R*-space used in this work will first be demonstrated in detail on the spectrum of the O_2-treated CZ-31−0.58 sample. Figure 3 displays the k^3-weighted raw EXAFS data of this sample. A very good signal-to-noise ratio is observed and the data are analyzed in the range 4 $Å^{-1} < k < 12$ $Å^{-1}$. Parts a−c of Figure 4 depict respectively the k^2-, k^0- and k^3-weighted Fourier transforms of these raw EXAFS data. Comparing different k^n-weighted Fourier transforms can be very informative as the backscattering amplitude and phase shift of each neighboring atom show a unique element specific dependency on the wavefactor *k*.

(44) Kharas, K. C. C.; Liu, D. J.; Robota, H. J. *Catal. Today* **1995**, *26*, 129.
(45) Kumashiro, P.; Kuroda, Y.; Nagao, M. *J. Phys. Chem. B* **1999**, *103*, 89.
(46) Kau, L. S.; Hodgson, K. O.; Solomon, E. I. *J. Am. Chem. Soc.* **1989**, *111*, 7103.
(47) Kau, L. S.; Spira-Solomon, D. J.; Penner-Hahn, J. E.; Hodgson, K. O.; Solomon, E. I. *J. Am. Chem. Soc.* **1987**, *109*, 6433.
(48) Koningsberger, D. C.; Mojet, B. L.; van Dorssen, G. E.; Ramaker, D. E. *Top. Catal.* **2000**, *10*, 143.

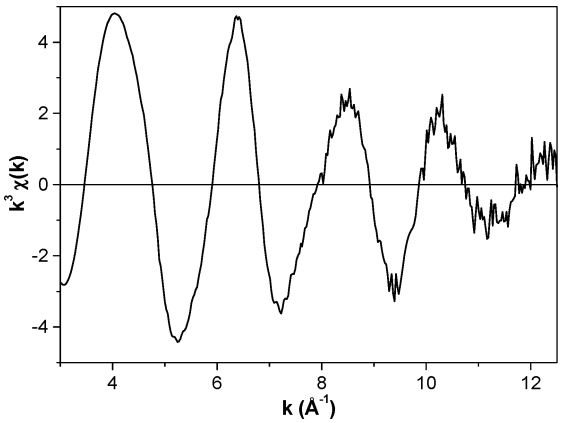

Figure 3. k^3-weighted raw EXAFS data of O_2-treated CZ-31−0.58.

Table 3. EXAFS Analysis Results for the CZ-31−0.58 and CZ-12−0.62 Samples Treated in O_2 at 623 K

					var	
Ab-Sc pair[a]	N[b]	R[c]	$\Delta\sigma^2$ [d]	ΔE_0[e]	im[f]	abs[g]
CZ-31−0.58, LN						
Cu−O	4.5	1.94	0.002	−3.2	k^0: 0.115	0.043
Cu···Cu	1.0	2.92	0.010	−3.5	k^3: 0.045	0.029
CZ-12−0.62, LN						
Cu−O	4.1	1.95	0.002	−5.0	k^0: 0.224	0.076
Cu···Cu	0.9	2.87	0.009	−2.0	k^3: 0.349	0.162
Cu···Al	0.8	3.21	0.006	−1.0		

[a] Ab = absorber; Sc = scatterer. [b] Coordination number. [c] Distance (Å). [d] Debye−Waller factor (Å^2). [e] Inner potential correction (eV). [f,g] Variances of the fit of the imaginary and absolute part, respectively. Fit: R-space, $4 < k < 12$ Å^{-1}; $1 < R < 3$ Å.

Comparing the raw data of Figure 4a−c shows that one major contribution can be distinguished in all spectra around 1.5 Å (without phase correction), while from ∼2 Å the Fourier transform pattern is different in each k^n-weighting. The latter observation points at the presence of constructive/destructive interferences between the different coordination shells. These results illustrate why an interpretation at the sight is not acceptable and an analysis should always include different k^n-weightings.[34] More specifically, a fit in one k^n-weighting is correct only if the other k^n-weightings yield minima in variances too.

First, the k^2-weighted spectrum of the O_2-treated CZ-31−0.58 sample was analyzed. In the range of $1.0 < R < 3.0$ Å the O and Cu shells were fitted by iteratively optimizing the parameters of each shell (N, coordination number; R, distance; $\Delta\sigma^2$, Debye−Waller factor; ΔE_0, inner potential correction). Table 3 shows that 4.5 oxygens were found at a distance of 1.94 Å and one copper atom at 2.92 Å. Table 3 also gives the fit variances of this result for k^0- and k^3-weighted spectra. Variances smaller than unity are obtained which proves the correctness of the fit. The quality of the fit can also be observed from Figure 4, showing the high match of the fit with the raw data for each k^n-weighting.

When the second shell was fitted with aluminum or oxygen instead of copper, no fit that is good for both k^0- and k^3-weighted spectra could be obtained, although a reasonable fit in either weighting could be obtained. Moreover, in the case of an aluminum neighbor, a reasonable fit could only be obtained with nonphysical (negative) values for the Debye−Waller factor. This finding shows that the used analysis method is able to distinguish

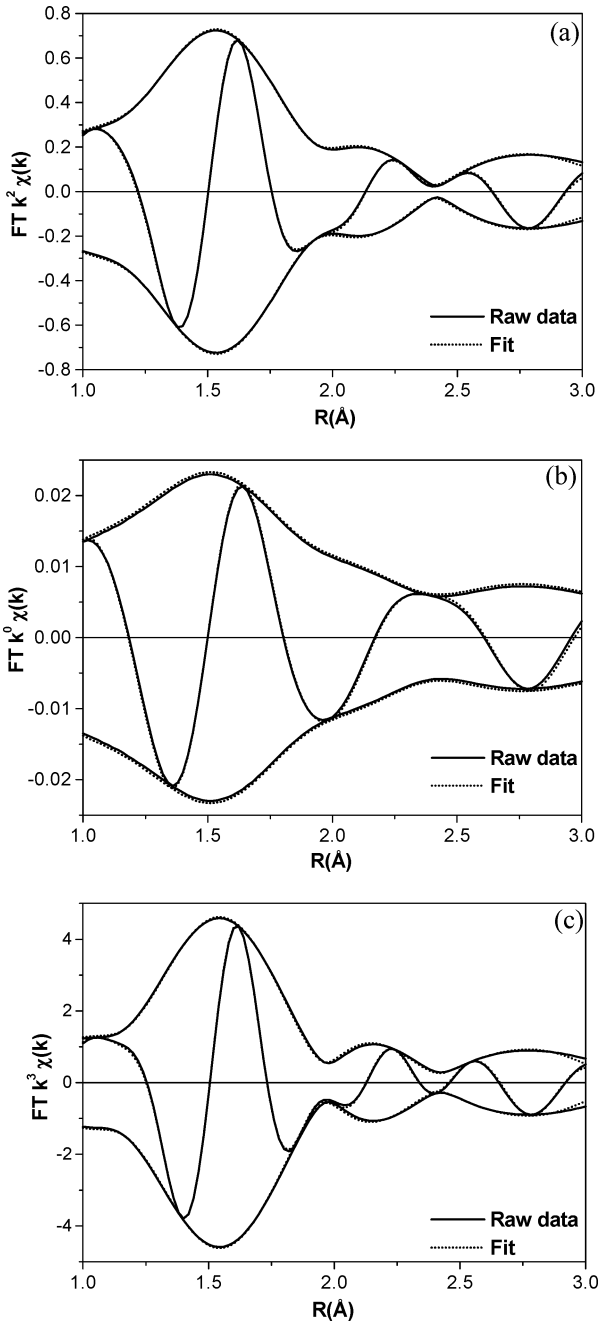

Figure 4. Fourier transforms of raw data and R-space fit ($4 < k < 12$ Å^{-1} and $1 < R < 3$ Å) of CZ-31−0.58 treated in O_2 at 623 K and measured at LN (a) k^2-, (b) k^0-, and (c) k^3-weighted.

copper from aluminum and oxygen. The underlying reason is that copper is a heavy scatterer that has significant backscattering amplitude at high k, whereas both aluminum and oxygen show strongly decreasing backscattering amplitude as a function of k. In this case, copper can be distinguished via both k^0- and k^3-weighting from the lighter scatterers. In Figure 5a the fit of the O shell is compared with its difference file, i.e. the raw data minus the fitted contribution of Cu. The analogue for Cu is depicted in Figure 5b. These figures show that the O and Cu shells are fitted well and that they are clearly above the noise. Finally, in Figure 6 the fitted Cu−O and Cu···Cu contributions are superimposed, illustrating the anti phase behavior of the O and Cu shells resulting in low intensity of the Fourier transform at 2.4 Å. This figure also proves the necessity of fitting, as the

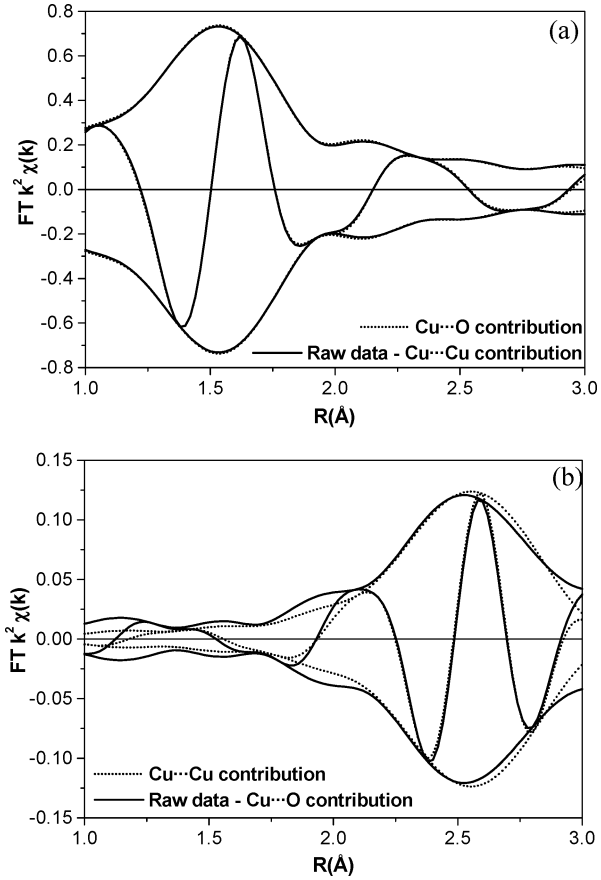

Figure 5. Fourier transforms of fitted single shell contributions (dotted line) and difference files (solid line) of *R*-space fit (k^2, $4 < k < 12$ Å^{-1}, and $1 < R < 3$ Å) of CZ-31−0.58 treated in O_2 at 623 K and measured at LN (a) Cu···O and (b) Cu···Cu.

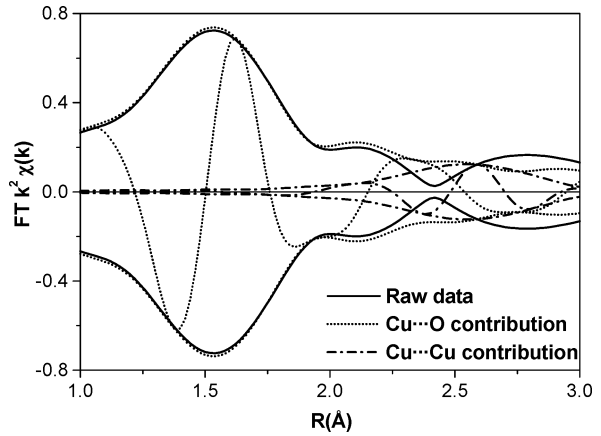

Figure 6. Fourier transforms of raw data and fitted single shell contributions of Cu···O and Cu···Cu of *R*-space fit (k^2, $4 < k < 12$ Å^{-1}, and $1 < R < 3$ Å) of CZ-31−0.58 treated in O_2 at 623 K and measured at LN.

Cu shell, peaking at 2.55 Å, can clearly not be detected by an interpretation by eye in neither *k*-weighting.

3.4. Fitting Results. The EXAFS parameters obtained for the O_2-treated CZ-12−0.62 sample are quite similar to those of the O_2-treated CZ-31−0.58 sample and are summarized in Table 3. The Cu−O contribution was also found at 1.95 Å but with a somewhat smaller coordination number of 4.1. For the Cu···Cu contribution a coordination number of 0.9 was obtained at a distance of 2.87 Å. At a distance of about 3.2 Å a light scatterer was found which could be well-fitted by aluminum.

Table 4. EXAFS Analysis Results of the CZ-12−0.62 Sample

Ab–Sc pair[a]	N[b]	R[c]	$\Delta\sigma^{2}$ [d]	ΔE_0 [e]	var im[f]	var abs[g]
CZ-12−0.62 treated in He at 393 K, measured at LN						
Cu−O	4.0	1.96	−0.001	−4.2	k^0: 0.122	0.063
Cu···Al	0.7	3.18	0.008	−12.6	k^3: 0.749	0.299
CZ-12−0.62 treated in He at 773 K, measured at 773 K						
Cu−O	2.3	1.92	0.006	2.7	k^0: 0.010	0.006
Cu···Cu	0.5	2.84	0.015	1.4	k^3: 0.170	0.082
CZ-12−0.62 in NO/He at 773 K, measured at 773 K						
Cu−O	3.4	1.92	0.008	−0.8	k^0: 0.377	0.095
Cu···Cu	1.4	2.79	0.017	6.8	k^3: 0.466	0.193
CZ-12−0.62 in NO/He at 773 K, measured at LN						
Cu−O	3.5	1.95	0.001	−4.6	k^0: 0.321	0.166
Cu···Cu	1.5	2.87	0.013	−1.0	k^3: 0.902	0.415

[a] Ab = absorber; Sc = scatterer. [b] Coordination number. [c] Distance (Å). [d] Debye−Waller factor (Å^2). [e] Inner potential correction (eV). [f,g] Variances of the fit of the imaginary and absolute part, respectively. Fit: *R*-space, $4 < k < 12$ Å^{-1}; $1 < R < 3$ Å.

The finding of a Cu···Cu coordination number close to 1 for both O_2-treated CZ-31−0.58 and CZ-12−0.62 samples automatically suggests the presence of dimeric copper species. However, knowing that EXAFS averages the local environments of all copper atoms, the latter coordination number could also result from a mixture of isolated and multimeric copper species. TEM micrographs were made of the O_2-treated CZ-31−0.58 sample in order to examine the presence of multimeric copper species. As no dark spots could be detected on the TEM photos, the presence of large copper oxide precipitates can be refuted. Consequently, the Cu···Cu contribution found in EXAFS must result from dimeric or oligomeric copper species.

Figure 7 depicts the k^2-weighted Fourier transforms of the raw data of the CZ-12−0.62 sample respectively after treatment (a) at 393 K in He, (b) at 773 K in He, (c) at 773 K in NO/He, and (d) at 773 K in NO/He and cooling the sample. The fits are presented in the respective figures, while the corresponding parameters are shown in Table 4. After treatment at 393 K, the first shell consists of a Cu−O contribution at 1.96 Å with a coordination number of 4. A second contribution at about 3.2 Å was found, which could only correctly be fitted with aluminum. Hence, the copper is exchanged as mononuclear copper into the zeolite. Dehydration in He at 773 K causes a serious reduction of the O coordination shell: only 2.3 oxygens at a distance of 1.92 Å were found. A second smaller contribution was found to correspond with 0.5 Cu at a distance of 2.84 Å. Upon admission of NO, the coordination number of the O shell increases up to 3.4, while its distance remains at 1.92 Å. However, it has to be noted that this increase in coordination number could also be due to nitrogen, as N and O are neighboring atoms in the periodic table, which makes them extremely difficult to distinguish. Also the Cu···Cu coordination number increases and amounts to 1.4. A somewhat smaller Cu···Cu distance of 2.79 Å is found in comparison with the 2.84 Å Cu···Cu separation in the dehydrated state. After prolonging the NO decomposition reaction and cooling the sample to LN, the coordination numbers of both the O and Cu shell are not much altered. On the other hand, both Cu−O and Cu···Cu coordination distances are lengthened and amount to 1.95 and 2.87 Å, respectively. Interestingly, this Cu···Cu coordination distance is identical to the Cu···Cu distance found after O_2-treatment (Table 3).

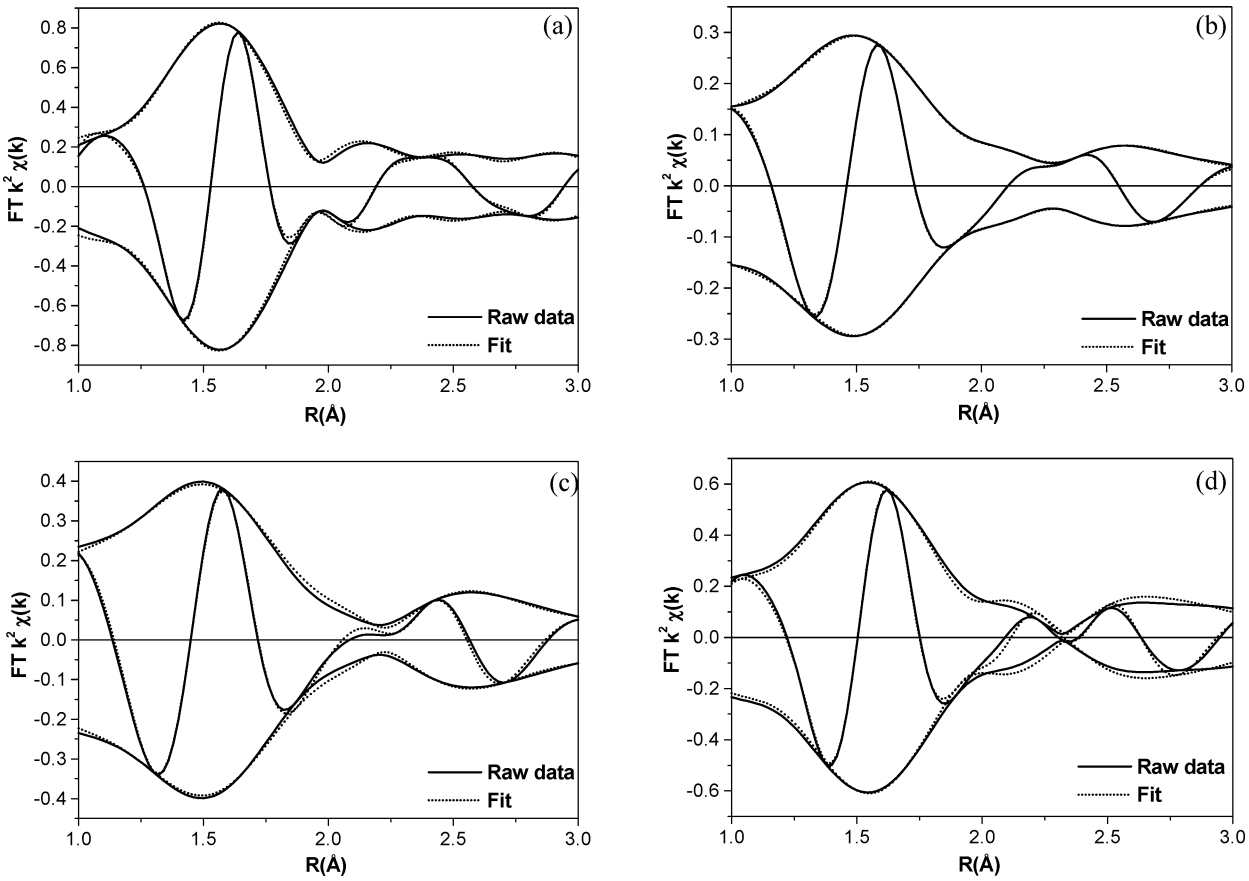

Figure 7. k^2-weighted Fourier transforms of raw data and *R*-space fit ($4 < k < 12$ Å^{-1} and $1 < R < 3$ Å) of CZ-12−0.62 after (a) treatment at 393 K in He and measured at LN, (b) treatment at 773 K in He and measured at 773 K, (c) treatment at 773 K in NO/He and measured at 773 K, and (d) treatment at 773 K in NO/He and measured at LN.

3.5. EPR and DRS. For each of the O_2-treated (at 623 K) samples, the amount of paramagnetic Cu(II) was determined by EPR and compared to its total (ICP) copper content. It was found that the calibrated spin concentration of O_2-treated CZ-31−0.16, CZ-31−0.34, and CZ-31−0.58 amounted respectively to 70, 33, and 19% of the total copper content. The two EPR signals characterizing the detectable fraction of copper atoms are generally assigned to isolated Cu(II) ions in the cation sites of the zeolite.[49−52] To gain more information on the fraction of EPR undetectable copper that grows with increasing Cu/Al ratio, UV−vis−near-IR measurements were performed on the same samples. Figure 8 shows the DRS spectra of O_2-treated CZ-31−0.16, CZ-31−0.34, and CZ-31−0.58. For the sample with Cu/Al ratio of 0.16, the spectrum is characterized by a d−d band centered at 13 400 cm^{-1} and a very intense charge-transfer (CT) band at 43 600 cm^{-1} with a small shoulder at about 28 000 cm^{-1}. In literature, the 13 400 and 43 600 cm^{-1} bands are assigned to respectively the d−d and CT O → Cu transitions of isolated Cu(II) ions in coordination with lattice oxygens.[21] After increasing the copper loading to Cu/Al ratio's of 0.34 and 0.58, additional bands at 6200, 9200, 22 700, and 30 000 cm^{-1} can be distinguished in both spectra. The finding that these four bands increase equally with copper loading, i.e., with the amount of EPR silent copper, supports the assumption that they originate from a single copper species. The concomitant presence of these four bands was also confirmed during stepwise dehydration. The hydrated CZ-31−0.58 sample was flushed with O_2, and the copper species according to this remarkable fingerprint spectrum was formed at 623 K and higher (with 823 K the highest temperature tested). UV−vis−near-IR spectra were also collected for CuO, $Cu(OH)_2$, and $Cu(CH_3CO_2)_2 \cdot H_2O$. The Cu−ZSM-5 fingerprint spectrum could not be explained by any of the latter compounds.

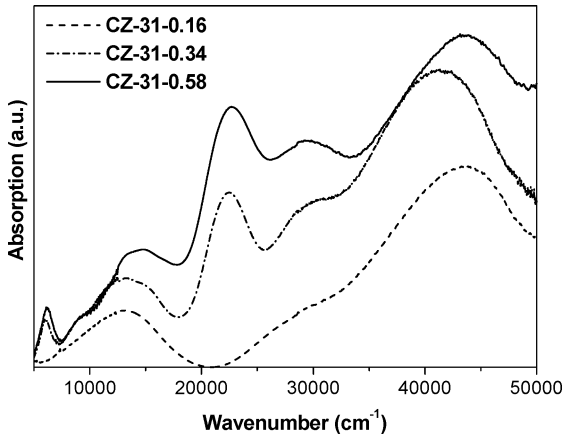

Figure 8. UV−vis−near-IR DRS spectra of O_2-treated (3 h at 623 K) CZ-31−0.16, CZ-31−0.34, and CZ-31−0.58.

(49) Delabie, A.; Pierloot, K.; Groothaert, M. H.; Schoonheydt, R. A.; Vanquickenborne, L. G. *Eur. J. Inorg. Chem.* **2002**, 515.
(50) Delabie, A.; Pierloot, K.; Groothaert, M. H.; Weckhuysen, B. M.; Schoonheydt, R. A. *Phys. Chem. Chem. Phys.* **2002**, *4*, 134.
(51) Dedecek, J.; Sobalík, Z.; Tvaružková, Z.; Kaucký, D.; Wichterlová, B. *J. Phys. Chem.* **1995**, *99*, 16327.
(52) Kucherov, A. V.; Slinkin, A. A.; Kondratev, D. A.; Bondarenko, T. N.; Rubinstein, A. M.; Minachev, K. M. *Zeolites* **1985**, *5*, 320.

4. Discussion

4.1. Identification of Bis(μ-oxo)dicopper in O_2-Treated Cu−ZSM-5. To investigate whether the UV−vis−near-IR fingerprint spectrum that characterizes the samples with $0.16 < Cu/Al \leq 0.6$ can be associated with the copper dimers suggested by the EXAFS results, a comparison was made with the thoroughly characterized Cu cores in enzymes and synthetic models. In homogeneous solution a number of complexes with 1:1, 2:1, 3:1, and 4:1 Cu/O_2 composition have been characterized both structurally and spectroscopically.[53] Inspecting the UV−vis spectra of these mono-,[54−59] di-,[60−62] tri-,[63] and tetranuclear[64] copper complexes showed that only for the dinuclear copper complexes a close correspondence with the spectrum of Cu−ZSM-5 is present. Three types of double-O-bridged Cu pairs are frequently encountered and classified by the structural arrangement of the Cu_2O_2 core atoms: bis(μ-oxo)dicopper, (μ-η^2:η^2-peroxo)dicopper, and trans(μ-1,2-peroxo)dicopper. A summary of the structural and spectroscopic characteristics of the first two complexes is presented in Table 5. The bis(μ-oxo)-dicopper isomer, i.e. $[Cu_2(\mu\text{-}O)_2]^{2+}$, was identified only in synthetic model complexes.[60,65−68] In this essentially planar Cu_2O_2 arrangement, the Cu···Cu distance amounts to 2.73−2.91 Å and the two bridging O atoms are widely separated. The bis(μ-oxo)dicopper core is EPR silent and exhibits a pair of intense CT bands ca. 22 300−25 000 and 30 800−32 700 cm^{-1}. The (μ-η^2:η^2-peroxo)dicopper core, i.e. $[Cu_2(\mu\text{-}\eta^2\text{:}\eta^2\text{-}O_2)]^{2+}$, constitutes the active site of the proteins hemocyanin, tyrosinase, and catechol oxidase in their oxidized forms.[69,70] But also in synthetic models this core arrangement could be obtained.[67,71] This isomer is identified by a Cu···Cu separation of about 3.5−3.8 Å, and a bridging peroxide (O_2^{2-}). The optical absorption spectrum is characterized by the peroxo → Cu(II) CT bands at about 17 000−19 800 and 27 300−29 600 cm^{-1}. Recently, also a "bent" or "butterfly" (μ-η^2:η^2-peroxo)dicopper geometry was characterized in synthetic models.[72] This bent geometry is distinguished from the planar variant by the presence of an additional CT band at 20 400−23 800 cm^{-1}. Finally, a trans(μ-1,2-peroxo)dicopper isomer with a Cu···Cu separation of more than 4 Å is observed in synthetic models[62] (not shown in Table 5).

Table 5. Summary of the Structural and Spectroscopic Properties of Cu−ZSM-5 and of Some Important Copper Pairs

	Cu-ZSM-5	$[Cu_2(\mu\text{-}O)_2]^{2+}$ bis(μ-oxo)-dicopper	$[Cu_2(\mu\text{-}\eta^2\text{:}\eta^2\text{-}O_2)]^{2+}$ (μ-η^2:η^2-peroxo)-dicopper	
			planar	bent 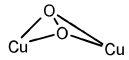
Cu-Cu[a]	2.79 - 2.92	2.73 - 2.91	3.5 – 3.8	3.2 - 3.4
O-O[a]		2.3	1.4	1.4
Cu-O[a]	1.95	1.79 - 1.89	1.7 - 2.2	
k_{max}[b]			17000 - 19800	~18200
ε[c]			~1000	~1000
k_{max}[b]	22700	22300 - 25000		20400 - 23800
ε[c]		13000 - 28000		~5000
k_{max}[b]	30000	30800 - 32700	27300 - 29600	~27800
ε[c]		11000 - 21000	~20000	~20000
Ref.		[60, 65-68]	[67, 69-71]	[72]

[a] Interatomic distances in Å. [b] k_{max} (the wavenumber of maximum absorption) in cm^{-1}. [c] ε (corresponding extinction coefficient) in M^{-1} cm^{-1}.

Inspection of the Cu···Cu separations of the different isomers in Table 5 shows that the bis(μ-oxo)dicopper isomer is the only possible candidate to explain the observed Cu···Cu separation of 2.79−2.92 Å of Cu−ZSM-5. The UV−vis spectrum of this bis(μ-oxo)dicopper core consists of an intense CT band at 22 300−25 000 cm^{-1} and a relatively weaker CT band at 30 800−32 700 cm^{-1}, in close agreement with the Cu−ZSM-5 spectrum, characterized by an intense band at 22 700 cm^{-1} and a weaker band at 30 000 cm^{-1}.

One could question the reliability of this comparison because in the synthetic models the bis(μ-oxo)dicopper core is surrounded by N-type ligands while in the zeolite only O-type ligands are available. We have two arguments in favor of our assignment. (1) In their DFT study, Goodman et al.[25] represented the zeolite environment by $[Al(OH)_4]^-$ tetrahedrons (to which Cu is 2-fold coordinated), and found three low-energy geometric isomers of the Cu_2O_2 core, i.e. bis(μ-oxo)dicopper, planar (μ-η^2:η^2-peroxo)dicopper, and trans(μ-1,2-peroxo)dicopper. (2) The O_{bridge} → Cu CT band maxima of bis(μ-oxo)dicopper are only slightly affected by the other ligands of Cu.[60]

The observed Cu···Cu separation of ~2.86 Å in the Cu−ZSM-5 samples falls in the upper range of the 2.73−2.91 Å separation in the bis(μ-oxo)dicopper complexes. This might be due to the negatively charged zeolite lattice that serves as bidentate ligand. So far, only a few bis(μ-oxo)dicopper cores with negatively charged ligands have been described, and these are also characterized by relatively long Cu···Cu separations.[68,73]

(53) Mahadevan, V.; Gebbink, R.; Stack, T. D. P. *Curr. Opin. Chem. Biol.* **2000**, *4*, 228.
(54) Fujisawa, K.; Tanaka, M.; Morooka, Y.; Kitajima, N. *J. Am. Chem. Soc.* **1994**, *116*, 12079.
(55) Wada, A.; Harata, M.; Hasegawa, K.; Jitsukawa, K.; Masuda, H.; Mukai, M.; Kitagawa, T.; Einaga, H. *Angew. Chem., Int. Ed.* **1998**, *37*, 798.
(56) Kitajima, N.; Morooka, Y. *Chem. Rev.* **1994**, *94*, 737.
(57) Wei, N.; Murthy, N. N.; Chen, Q.; Zubieta, J.; Karlin, K. D. *Inorg. Chem.* **1994**, *33*, 1953.
(58) Spencer, D. J. E.; Aboelella, N. W.; Reynolds, A. M.; Holland, P. L.; Tolman, W. B. *J. Am. Chem. Soc.* **2002**, *124*, 2108.
(59) Schatz, M.; Becker, M.; Thaler, F.; Hampel, F.; Schindler, S.; Jacobson, R. R.; Tyeklár, Z.; Murthy, N. N.; Ghosh, P.; Chen, Q.; Zubieta, J.; Karlin, K. D. *Inorg. Chem.* **2001**, *40*, 2312.
(60) Que, L.; Tolman, W. B. *Angew. Chem., Int. Ed.* **2002**, *41*, 1114.
(61) Jacobson, R. R.; Tyeklár, Z.; Farooq, A.; Karlin, K. D.; Liu, S.; Zubieta, J. *J. Am. Chem. Soc.* **1988**, *110*, 3690.
(62) Tyeklár, Z.; Jacobson, R. R.; Wei, N.; Murthy, N. N.; Zubieta, J.; Karlin, K. D. *J. Am. Chem. Soc.* **1993**, *115*, 2677.
(63) Cole, A. P.; Root, D. E.; Mukherjee, P.; Solomon, E. I.; Stack, T. D. P. *Science* **1996**, *273*, 1848.
(64) Reim, J.; Werner, R.; Haase, W.; Krebs, B. *Chem.-Eur. J.* **1998**, *4*, 289.
(65) Halfen, J. A.; Mahapatra, S.; Wilkinson, E. C.; Kaderli, S.; Young, V. G.; Que, L.; Zuberbühler, A. D.; Tolman, W. B. *Science* **1996**, *271*, 1397.
(66) Tolman, W. B. *Acc. Chem. Res.* **1997**, *30*, 227.
(67) Holland, P. L.; Tolman, W. B. *Coord. Chem. Rev.* **1999**, *192*, 855.
(68) Aboelella, N. W.; Lewis, E. A.; Reynolds, A. M.; Brennessel, W. W.; Cramer, C. J.; Tolman, W. B. *J. Am. Chem. Soc.* **2002**, *124*, 10660.
(69) Solomon, E. I.; Sundaram, U. M.; Machonkin, T. E. *Chem. Rev.* **1996**, *96*, 2563.
(70) Eicken, C.; Zippel, F.; Büldt-Karentzopoulos, K.; Krebs, B. *FEBS Lett.* **1998**, *436*, 293.
(71) Kitajima, N.; Fujisawa, K.; Fujimoto, C.; Morooka, Y.; Hashimoto, S.; Kitagawa, T.; Toriumi, K.; Tatsumi, K.; Nakamura, A. *J. Am. Chem. Soc.* **1992**, *114*, 1277.
(72) Pidcock, E.; Obias, H. V.; Abe, M.; Liang, H. C.; Karlin, K. D.; Solomon, E. I. *J. Am. Chem. Soc.* **1999**, *121*, 1299.

More specifically, Cu···Cu separations of 2.85 and 2.91 Å have been found for bis(μ-oxo)dicopper cores with one[68] and two[73] anionic ligands, respectively. Second, a comparison of the Cu−O shell of the studied zeolite samples with the Cu−O bond distances in the Cu_2O_2 core is not that evident since, (i) in the zeolite, each copper ion is expected to bind in addition oxygen atoms of the lattice and (ii) also the fraction of isolated Cu(II) ions partly determines the Cu−O EXAFS analysis results. In an ab initio study by our group,[50] the isolated Cu(II) ions were found to coordinate four or five lattice oxygens at a distance of 1.9 to 2.4 Å. Consequently, the EXAFS Cu−O coordination number of 4.1−4.5 and the distance of 1.94−1.95 Å can be explained by an average of (i) longer and shorter Cu−O bonds respectively with zeolite oxygen and extralattice oxygen and (ii) 4-fold and 4-/5-fold Cu−O coordinations respectively in the bis(μ-oxo)dicopper cores and monomers.

One argument often raised against the existence of copper pairs in Cu−ZSM-5 is the fact that two Al sites in close enough proximity to charge-balance copper dimers is unlikely in this highly siliceous zeolite. However, using Monte Carlo simulations, Goodman et al.[74] determined that, for the typical Si/Al ratios of ZSM-5, the probability of a given Al site having at least one suitable Al partner for pairing within 8.5 Å is close to unity. Moreover, they showed that, due to its specific zeolite structure, ZSM-5 has a higher probability of short-distance (r < 5.5 Å) Al pairs, supporting puckered Cu oxocations,[75] than either ferrierite or mordenite.

Ab initio calculations[25,60,76,77] showed that the bis(μ-oxo)dicopper isomer has a singlet ground state, explaining the lack of an EPR signal. A comment concerning the quantity of these copper pairs can be made when comparing the EXAFS Cu···Cu coordination number of 1.0 with the EPR silence of about 81% of the copper in CZ-31−0.58. Taking into account the margins of error of both techniques, a quite good match is observed. On the other hand, it cannot be ruled out that besides the mononuclear copper and the bis(μ-oxo)dicopper cores, also a smaller fraction of oligomeric copper might be present.

Generally, a formal Cu(III) oxidation state is assigned to the bis(μ-oxo)dicopper core.[60] However, the position of the 1s → 3d preedge peak at 8977.5 eV in the XANES spectrum of Cu−ZSM-5 (Figure 2b,c) indicates that the actual charge on copper is less than 3-fold positive,[78] which can be due to the 2-fold negative charge of the zeolite oxygen ligands. Additionally, this observation that the actual charge on copper might be closer to 2-fold than 3-fold positive in the bis(μ-oxo)dicopper core of Cu−ZSM-5 is supported by a bond valence sum (BVS) analysis[60,77] (see Table S2 of the Supporting Information). On the basis of this quantitative relationship, the relatively longer Cu···Cu separation and concomitant longer copper−ligand bond distances in this and a second neutral bis(μ-oxo)dicopper core[73] are consistent with a lower oxidation state in comparison to the complexes with shorter Cu···Cu separations.[60,77]

So far, the bis(μ-oxo)dicopper complex has only been synthesized in homogeneous solutions at temperatures < −40 °C.[60] This low temperature is necessary to prevent hydrogen abstraction of the ligands or of the solvent by the O-bridges, resulting in the formation of the bis(μ-hydroxo)dicopper complex. Regarding the zeolite samples, the bis(μ-oxo)dicopper core can be observed at much higher temperatures. However, traces of water cause the immediate disappearance of the 22 700 cm^{-1} band, and thus of the bis(μ-oxo)dicopper complex, while an absorption band ca. 30 000 cm^{-1} remains. This observation conforms with the formation of bis(μ-hydroxo)dicopper as the latter core exhibits a (OH → Cu) CT band in the range 30 000−32 000 cm^{-1}.[70,79]

In summary, it can be concluded that the close correspondence of spectroscopic and structural characterizations strongly suggests the presence of bis(μ-oxo)dicopper in the O_2-treated overexchanged Cu−ZSM-5 zeolite. Resonance Raman spectra, acquired via laser excitation into the 22 700 cm^{-1} band, could offer additional important confirmation for the assignment of this UV−vis band of the Cu−ZSM-5 sample to the bis(μ-oxo)-dicopper structure. However, the low copper content of the Cu−ZSM-5 sample together with its air-sensitivity and fluorescence ability prohibited the measurements to date.

The latter assignment is in contrast with the current interpretation,[20−23] which attributes the 22 700 cm^{-1} band to a single-O-bridged Cu pair, i.e. $[CuOCu]^{2+}$. To the best of our knowledge, single-O-bridged Cu pairs are less common than double-O-bridged Cu pairs after O_2 activation—at least in organometallic and bio-inorganic chemistry—and they give rise to CT bands in the 30 000−40 000 cm^{-1} range, rather than at 22 700 cm^{-1}.[80] The present identification might seem to contradict the mass spectrometric results of Iglesia and co-workers,[16] which are consistent with single-O-bridged Cu pairs in O_2-treated Cu−ZSM-5. However, Iglesia and co-workers observed H_2 consumption by Cu−ZSM-5 at 450 K, whereas we found bis(μ-oxo)dicopper reacting with H_2 at RT, which indicates that different copper species were investigated in both studies. This can be due to a different O_2-treatment procedure, and we stress that, in order to stabilize the bis(μ-oxo)dicopper core in Cu−ZSM-5, cooling should be done in O_2 atmosphere. We also want to emphasize that the identification of bis(μ-oxo)-dicopper in O_2-treated Cu−ZSM-5 does not exclude the presence of single-O-bridged Cu pairs in Cu−ZSM-5 after other pretreatments.

The importance of a correct understanding of the copper core in the overexchanged Cu−ZSM-5 is nicely illustrated when we combine the results of Iwamoto et al.[6] with ours. In their study of the NO decomposition activity of Cu−ZSM-5 as a function of the Cu/Al ratio, they observed a very sharp increase in activity near Cu/Al = 0.2. Fascinatingly, we observed that the bis-(μ-oxo)dicopper core is not yet formed in a sample with Cu/Al = 0.16 but is present in a sample with Cu/Al = 0.34. This concomitant occurrence of catalytic activity and the presence of the bis(μ-oxo)dicopper core is striking and strongly suggests a correlation.

(73) Straub, B. F.; Rominger, F.; Hofmann, P. *Chem. Commun.* **2000**, 1611.
(74) Goodman, B. R.; Hass, K. C.; Schneider, W. F.; Adams, J. B. *Catal. Lett.* **2000**, *68*, 85.
(75) Goodman, B. R.; Hass, K. C.; Schneider, W. F.; Adams, J. B. *J. Phys. Chem. B* **1999**, *103*, 10452.
(76) Flock, M.; Pierloot, K. *J. Phys. Chem. A* **1999**, *103*, 95.
(77) Mahapatra, S.; Halfen, J. A.; Wilkinson, E. C.; Pan, G. F.; Wang, X. D.; Young, V. G.; Cramer, C. J.; Que, L.; Tolman, W. B. *J. Am. Chem. Soc.* **1996**, *118*, 11555.
(78) DuBois, J. L.; Mukherjee, P.; Stack, T. D. P.; Hedman, B.; Solomon, E. I.; Hodgson, K. O. *J. Am. Chem. Soc.* **2000**, *122*, 5775.
(79) Karlin, K. D.; Hayes, J. C.; Gultneh, Y.; Cruse, R. W.; McKown, J. W.; Hutchinson, J. P.; Zubieta, J. *J. Am. Chem. Soc.* **1984**, *106*, 2121.
(80) Sanyal, I.; Mahroof-Tahir, M.; Nasir, M. S.; Ghosh, P.; Cohen, B. I.; Gultneh, Y.; Cruse, R. W.; Farooq, A.; Karlin, K. D.; Liu, S.; Zubieta, J. *Inorg. Chem.* **1992**, *31*, 4322.

4.2. Formation of Bis(μ-oxo)dicopper during NO Decomposition. Before NO decomposition experiments were started, the catalyst was dehydrated in a He flow at elevated temperature. The XANES and EXAFS results show that the effect of this pretreatment is 2-fold. First, the positions of the near-edge absorption features in the XANES spectra indicate that all Cu(II) is reduced to Cu(I) during treatment in He at 773 K (Figure 2c). Second, no significant Cu···Cu interaction could be distinguished in the EXAFS spectrum of the sample treated at 393 K, whereas a Cu···Cu coordination number of 0.5 is found after pretreatment at 773 K (Table 4). The most obvious explanation is that mononuclear Cu(II) enters the zeolite during the ion exchange procedure and that a mixture of Cu(I) monomers and Cu(I) pairs is formed during dehydration in He. In a recent DFT study of Sauer and co-workers, it was shown that, notwithstanding their formal charge and closed shell d^{10} electronic configuration, Cu(I) ions can indeed form pairs in Cu−ZSM-5, provided that Al atoms are present at appropriate framework positions.[81] The calculated Cu···Cu distances fall into the range 2.5−2.9 Å, which is in agreement with the observed Cu···Cu separation of 2.84 Å in this work. During NO decomposition at 773 K, Cu(I) is partly oxidized to Cu(II) as indicated by the XANES near-edge features (Figure 2c). Concomitantly, an increase of the Cu−O coordination number from 2.3 to 3.4 is observed in EXAFS (Table 4). Concerning the Cu···Cu coordination shell, a major increase in the coordination number from 0.5 to 1.4 is observed. Cooling down the sample to LN does not affect the coordination numbers, but a lengthening of the coordination distances is observed. Interestingly, the Cu···Cu separation amounts to 2.87 Å, which is identical to the Cu···Cu separation in the corresponding (CZ-12−0.62) O_2-treated sample, also measured at LN (Table 3). Moreover, also the XANES Cu(II) 1s → 3d and Cu(II) 1s → $4p_z$ + L → Cu(II) peak positions of the O_2-treated and reacted sample show a very close match (Figure 2b,c). This information strongly suggests the formation of the bis(μ-oxo)dicopper core during NO decomposition. While bis(μ-hydroxo)dicopper cores are characterized by quite similar Cu···Cu separations of 2.9−3.0 Å,[77] their formation is excluded since no H atoms are provided under these conditions. As the Cu···Cu coordination number clearly exceeds the value of 1 but the Cu···Cu separation stays invariant, it might be suspected that the bis(μ-oxo)dicopper cores aggregate into small chains. The formation of the bis(μ-oxo)dicopper core during NO decomposition was also proved using in situ optical fiber UV−vis spectroscopy. In this contribution of our group,[82] the role of the bis(μ-oxo)dicopper core was clearly derived using a combination of in situ UV−vis monitoring and on line GC analysis. This study shows that the bis(μ-oxo)dicopper core is formed by O-abstraction of N_2O and that it fulfills the key functions of O_2 production and release. The key role of the bis(μ-oxo)dicopper core was additionally proved by the fact that copper−mordenite (Si/Al = 5), on which bis(μ-oxo)dicopper could not be stabilized, showed a much lower NO decomposition activity (after contacting 1 mol % NO in He for 2 h at 773 K at 900 h^{-1} GHSV: the N_2 yield amounts to (i) <2% for Cu-MOR and (ii) 77 and 68% for CZ-31−0.58 and CZ-12−0.62, respectively).

Scheme 1. Role of Bis(μ-oxo)dicopper in the Catalytic NO Decomposition

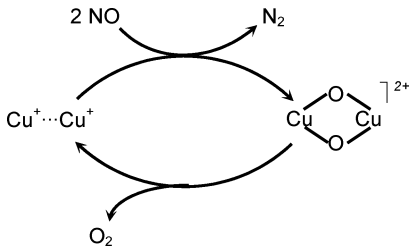

4.3. Role of Bis(μ-oxo)dicopper in the Catalytic Decomposition of NO. In accordance with the in situ XAFS results, Scheme 1 shows the role of bis(μ-oxo)dicopper in the catalytic NO decomposition. A $Cu^+\cdots Cu^+$ pair reacts with two NO molecules resulting in the formation of N_2 and bis(μ-oxo)-dicopper, which reconstitutes the $Cu^+\cdots Cu^+$ pair after desorption of O_2. In our combined in situ UV−vis−GC study[82] we reported that the first step in Scheme 1 consists of two consecutive steps: i.e. (i) the reaction of two NO molecules with $Cu^+\cdots Cu^+$ forming N_2O and $[CuOCu]^{2+}$ and (ii) the reaction of N_2O with $[CuOCu]^{2+}$ forming N_2 and bis(μ-oxo)-dicopper. The latter step is retarded below 623 K, causing the N_2O yield at these lower temperatures.

In the elaborate kinetic study of Li and Hall[41] it was concluded that the self-reduction of the catalytic sites by the desorption of O_2 is rate determining at 773 K. This conclusion can be shared by the present results as both the XANES and EXAFS data point at the presence of a considerable fraction of the bis(μ-oxo)dicopper core during NO decomposition. Li and Hall[41] also discussed that the removal of the strongly adsorbed product oxygen from the surface limits the NO decomposition on most catalysts. Therefore, the bis(μ-oxo)dicopper complex in Cu−ZSM-5 fulfills the key role of continuous O_2 production and release during steady-state reaction and in this way guarantees the sustained high activity of Cu−ZSM-5. Finally, the suitability of the bis(μ-oxo)dicopper core for the O_2 release function can be explained by the fact that this core can interconvert with its peroxo-isomer,[65,83] (μ-η^2:η^2-peroxo)dicopper (Table 5), which reversibly binds O_2 in the protein hemocyanin, the dioxygen carrier protein found in arthropods and mollusks.[84]

5. Conclusions

The presence of the bis(μ-oxo)dicopper core, i.e. $[Cu_2(\mu\text{-}O)_2]^{2+}$, in O_2-activated overexchanged Cu−ZSM-5 has been identified with UV−vis and EXAFS spectroscopies. The in situ XAFS spectra strongly support the formation of this $[Cu_2(\mu\text{-}O)_2]^{2+}$ core during direct NO decomposition. These results lead to a reaction cycle involving a $Cu^+\cdots Cu^+$ pair and the $[Cu_2(\mu\text{-}O)_2]^{2+}$ core. Heretofore, the presence of double-O-bridged Cu pairs in Cu−ZSM-5 was only postulated on the basis of the theoretical study of Goodman et al.[25] With the current contribution we have strong experimental evidence for the formation of the bis(μ-oxo)dicopper core in Cu−ZSM-5 and

(81) Spuhler, P.; Holthausen, M. C.; Nachtigallová, D.; Nachtigall, P.; Sauer, J. *Chem.-Eur. J.* **2002**, *8*, 2099.
(82) Groothaert, M. H.; Lievens, K.; van Bokhoven, J. A.; Battiston, A. A.; Weckhuysen, B. M.; Pierloot, K.; Schoonheydt, R. A. *ChemPhysChem* **2003**, in press.
(83) Mahadevan, V.; Henson, M. J.; Solomon, E. I.; Stack, T. D. P. *J. Am. Chem. Soc.* **2000**, *122*, 10249.
(84) Solomon, E. I.; Lowery, M. D. *Science* **1993**, *259*, 1575.

for its role in the sustained high activity of Cu−ZSM-5 in the direct decomposition of NO into N_2 and O_2.

So far, the bis(μ-oxo)dicopper core had only been characterized in synthetic complexes in solution. The latter homogeneous catalysts are capable of selectively oxidizing organic functional groups and of isomerizing to the (μ-η^2:η^2-peroxo)dicopper core, which constitutes the active site in the enzymes hemocyanin, tyrosinase, and catechol oxidase. Therefore, the anchoring of the bis(μ-oxo)dicopper complex on a solid matrix in this work might inspire future research to explore its abilities in heterogeneous selective oxidation catalysis.

Acknowledgment. Cor van der Spek is kindly acknowledged for the performance of the TEM measurements. We thank the Hamburger Synchrotronstrahlungslabor for the provision of synchrotron radiation and the personnel of Beamline X1.1 for their assistance during the X-ray absorption measurements (Project No. I-00-063 EC). This investigation has been supported by grants from the National Fund for Scientific Research—Flanders (FWO) and from the Concerted Research Action of the Flemish Government (GOA). M.H.G. thanks the Institute for the Promotion of Innovation by Science and Technology in Flanders (IWT) for a Ph.D. grant.

Supporting Information Available: Tables illustrating the accuracy of the EXAFS analysis method and the bond valence sum (BVS) analysis. This material is available free of charge via the Internet at http://pubs.acs.org.

JA029684W